

Dry, preloaded NANOR[®]-type CF/LANR components

Mitchell R. Swartz^{1,*}, Gayle M. Verner¹, Jeffrey W. Tolleson¹ and Peter L. Hagelstein²

¹JET Energy, Inc., Wellesley, MA 02481, USA

²Massachusetts Institute of Technology, Cambridge, MA02139, USA

Dry, preloaded NANOR[®]-type technology makes LANR reactions more accessible. These self-contained, two-terminal nanocomposite ZrO₂-PdNiD CF/LANR components have at their core ZrO₂-PdD nanostructured material. The excess energy gain compared to driving input energy is up to 20 times the input; characterized by reasonable reproducibility and controllability. The CF/LANR/CF activation is separated from its loading. Although small in size, the LANR excess power density is more than 19,500 W/kg of nanostructured material, with zero carbon footprint.

Keywords: Cold fusion, excess energy, nanomaterial, preloading.

Aqueous cold fusion augmented by nanomaterials

LATTICE assisted nuclear reactions [LANR, also known as cold fusion (CF) and LENR] use hydrogen-loaded alloys to generate heat and other products¹⁻³ by enabling deuterium fusion to form an excited *de novo* helium nucleus at near-room temperature under difficult-to-achieve conditions. The 'excess heat' observed is thought due to energy derived from coherent de-excitation of molecule D₂ to ground state ⁴He, with the large 24 MeV quantum fractionated into optical phonon vibrations near 65 meV. Usually, in the past, successful LANR required engineering of multiple factors including loading, adequate confinement time, loading rate and prehistory (with careful avoidance of contamination and materials and operational protocols which quench performance). Today, dry, preloaded NANOR[®]-type technology makes LANR more accessible.

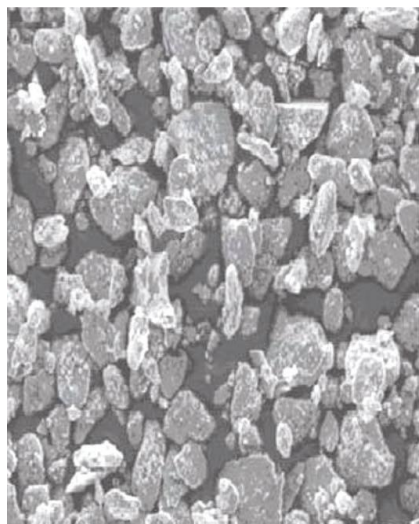
Nanostructured materials are important in LANR and are also produced in codeposition structures, observed producing non-thermal near-infrared emissions when active, and exhibit typical CF/LANR excess heat correlated with the size of the Pd-D nanostructures². These self-contained, two-terminal nanocomposite ZrO₂-PdNiD CF/LANR components feature new composition, struc-

ture and superior handling properties enabling portability and transportability and are capable of significant reproducible energy gain^{4,5} (Figure 1). The NANOR[®] components are smaller than 2 cm in length, and with 30–200 mg of active LANR material. Their 'core' contains active ZrO₂-PdD nanostructured material⁶, loaded with additional D to loadings (ratio of D to Pd) of more than 130%, but shallow traps are not ruled out because palladium nanoparticles often have a vacancy in their centre⁷ and vacancies within them. Bulk PdD is one of the most studied metal deuterides, with deuterium in the octahedral sites at high D/Pd loading near unity. Nano-scale Pd occurs in the Fm3m space group, while bulk Pd is FCC; the miscibility gap for nano PdD is narrower than for bulk PdD; and the solubility is a bit lower for the nano PdD. In some crystals, Pd²⁺ ion is observed and is paramagnetic. The ZrO₂-(PdNi)D is prepared in a complicated process that begins by oxidizing a mixture of zirconium oxide surrounding metallic palladium, nickel or Pd-Ni islands. The sudden glassy freezing of the molten alloy produces an amorphous, metal, tinsel, ribbon foil of size ~0.5 mm × 2 to 20 mm × ~0.1 mm thick; silver-coloured, shiny bright and smooth². After serial baking^{2,4} there is separation of the alloy into 7–10 nm sized, now ferromagnetic, nanostructured islands located and dispersed within the electrically insulating zirconia dielectric. The material feels like crushed bituminous coal with complex electrical and magnetic properties.

For these NANOR[®]-type LANR components, the fuel for the nanostructured material in the core is deuterium; and the product is believed to be *de novo* ⁴He based upon previous aqueous studies³. These reactions are driven and activated by an applied electrical current. Most importantly, they are pre-loaded so that LANR activation is separated from the loading. In every other system known, Fleischmann and Pons, Arata, Miles, etc. the loading has been tied to activation at room temperature. It is a long, expensive, arduous effort to prepare these preloaded nanocomposite CF/LANR components, but by contrast, these can be simply electrically driven.

LANR (CF)-activated nanocomposite ZrO₂-PdNiD and ZrO₂-PdD CF/LANR quantum electronic components are capable of significant energy gain^{4,5}, with significant

*For correspondence. (e-mail: mica@theworld.com)



For verification, the energy gains were confirmed by three methods and by time integration. The calorimeter had parallel diagnostics, including heat-flow measurement, and calibrations included an ohmic (thermal) control located next to the NANOR[®]-type device.

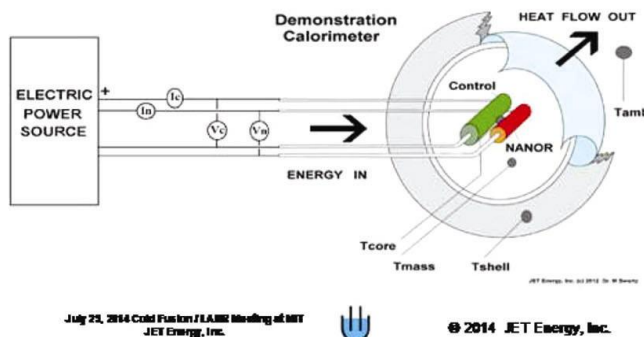


Figure 1. Nanostructured material (left) and its stereoconstellation with the ohmic (thermal) control in the excess heat experiments. The large central thermal mass is not shown here.

improvement over all of their predecessors in sustained activity, including the highly successful metamaterial PHUSOR[®]-type of LANR component. They have been carefully evaluated for energy gain, including during and after the January 2012 IAP MIT course on CF/LANR. The excess energy gain compared to driving input energy is up to 20 times (sometimes more).

The first publicly shown NANOR[®]-type LANR component appeared during and after the January 2012 IAP MIT course on CF/LANR. It demonstrated energy gain which ranged generally from 5 to 16. Energy gain was 14.1 while the MIT IAP course was ongoing; and other NANORs have demonstrated higher gain. The 2012 Open LANR/CF Demonstration at MIT had parallel diagnostics, including calorimetry, input-power-normalized ΔT , and focused heat flow measurement (such as Omega HFS Thin Film) and calibration with an ohmic (thermal) control located next to the NANOR[®]. The NANOR and the thermal control are at the centre of much larger thermal mass in the calorimeter, discussed in more detail elsewhere^{4,5}.

Electrical activation of NANOR[®]-type CF/LANR component

The LANR preloaded, stabilized NANORs were driven by a high DC voltage circuit up to 1000⁺ V rail voltage. The duty cycle was split with half going to a control portion consisting of a carefully controlled electrical DC pulse into an ohmic resistor which was used to thermally calibrate the calorimeter⁴. Data acquisition was taken from voltage, current and temperatures at multiple sites of the solution, and outside of the cell. Data acquisition sampling was done at data rates of 0.20 to 1 Hz, with 24+ bit resolution; voltage accuracy 0.015^{±0.005} V and temperature accuracy <0.6°C). The noise power of the calorimeter was in the range ~1–30 mW. The noise power of

the Keithley current sources is generally ~10 nW. Input power is defined as $V \cdot I$. There is no thermoneutral correction in the denominator. Therefore, the observed incremental power gain is actually a lower limit.

The result is heat measurement of this preloaded NANOR[®]-type LANR device by three ways, ending in calorimetry, input-power-normalized ΔT (dT/P_{in}), and input power normalized heat^{4,5} (HF/P_{in}). These three methods of verification are pooled to derive useful information, including the energy produced ('excess energy') and sample activity.

The instantaneous power gain (power amplification factor (non-dimensional)) is defined as P_{out}/P_{in} . The energy is calibrated by at least one electrical joule control (ohmic resistor) used frequently, and with time integration for additional validation. The excess energy, when present, is defined as $[P_{output} - P_{input}] \times \text{time}$. The amount of output energy (and therefore, both power and energy gain) is determined from the heat released producing a temperature rise, which is then compared to the input energy. The output of the NANOR is compared to the output of the precisely driven ohmic control.

The NANOR[®]-type preloaded LANR component openly demonstrated energy gain (COP) which ranged generally from 5 to 16 (e.g. 14.1 (~1412%) while the MIT IAP course was ongoing⁵). It had a much higher energy gain compared to the 2003 demonstration unit (energy gain 14.1 in 2012 vs ~2.7 in 2003).

The input powers were below 100 mW^{4,5}, because the set-up was designed to run at low power input levels to increase safety for its multi month-long stay at MIT. There were daily calibrations using input current and voltage standards. In this case, low power was used for several reasons, including to facilitate the rapid time constant and because this is for demonstration and teaching purposes. More recently, these NANOR[®]-type components have been driven up to the 2 W level.

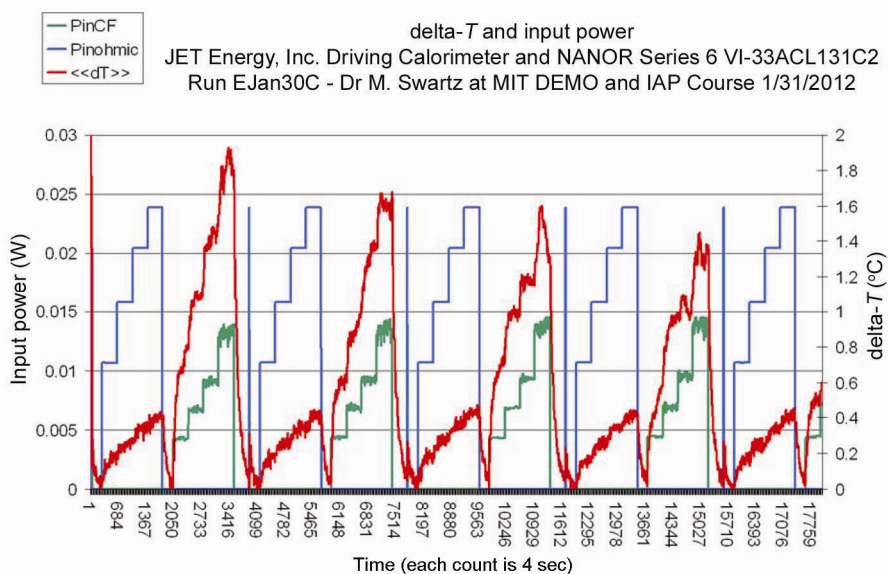


Figure 2. Input power and incremental output temperature rise of a self-contained CF/LANR quantum electronic series VI NANOR[®] device. These curves plot the raw data as incremental temperature rise and the applied input electrical power as the power is switched between an ohmic (thermal) control and the CF/LANR component, alternatively. There is a pair of calibration pulses between each set.

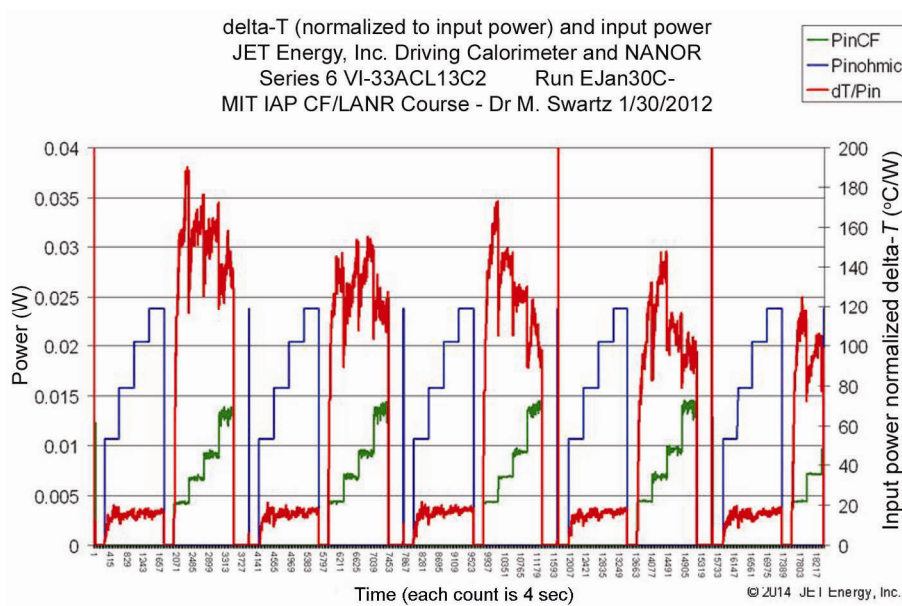


Figure 3. Plot showing temperature rise (delta-T , °C) of the ohmic control and the preloaded NANOR[®]-type LANR device, both normalized to input electrical power. Shown are the input power (left-hand axis) and resulting output temperature rise normalized to input electrical power (right-hand axis). Next to the control resistor is the self-contained CF/LANR quantum electronic component, a series VI two-terminal NANOR[®]-type device containing active preloaded $\text{ZrO}_2/\text{PdNiD}$ nanostructured material at its core.

Figures 2–5 show this entirely new, more reproducible, much more powerful configuration of clean, efficient energy production from several points of view. The figures include raw data (Figure 2) and derived information from the runs which shows conclusively LANR excess energy. This is heralded by input power normalized incremental temperature (delta-T) changes and heat flow (Figures 3 and 4) and by calorimetry (Figure 5). These graphs shows

a small portion of the collected data and derived information which was actually collected and analysed by the class, and later in a four-month interval at MIT and many more months of study. They show the data collected from NANOR VI-33ACL131C2 with the incremental power gain determination by dT/P_{in} as 1096%, by HF/P_{in} as 1103%, and by calorimetry as 993%. The time-integrated energy gain was slightly less at 7.92. This indicates that

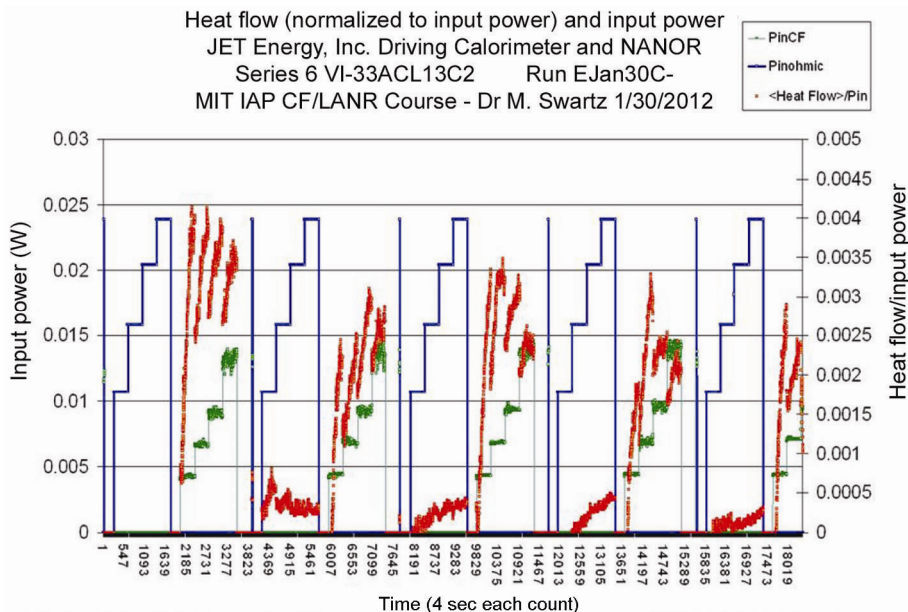


Figure 4. Input power and output heat flow normalized to input electrical power of a self-contained CF/LANR quantum electronic component.

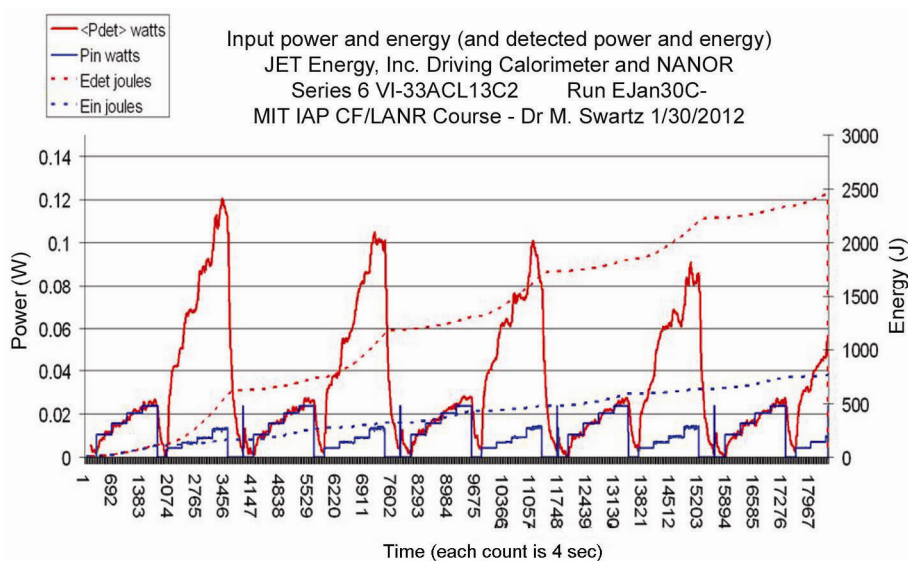


Figure 5. Input and heat output of a two-terminal NANOR[®]-type device series 6-33 device, showing the calorimetric response at several input powers, for the ohmic control and the component. Four complete cycles are shown.

the curves (Figures 2–5) herald documented excess energy of 1594.9 J.

Figure 2 demonstrates the excess heat from this component versus an ohmic control. Shown is the input power and incremental output temperature rise of a self-contained CF/LANR quantum electronic series VI NANOR[®] component. These curves plot the raw data as incremental temperature rise and the applied input electrical power as the power is switched between an ohmic (thermal) control and the CF/LANR component, alternatively. There is a pair of calibration pulses between each set. Figure 2 is a set of

curves which plot the differential incremental increase in temperature (°C) for the case with no input (‘background’), and for the case of an ohmic thermal control at the same location and the NANOR[®]-type LANR component. The graph in Figure 2 presents several curves which plot the temperature rise in response to four different levels of electrical input power, and the response of an ohmic control to same electrical input power. The x-axis represents time, and each count represents 4 sec. The y-axis on the left side represents electrical input power (in watts). The y-axis on the right side represents the temperature rise (differential

temperature increase) in response to the electrical input power ($^{\circ}\text{C}$). The input to the thermal ohmic control is shown, followed by the preloaded NANOR[®]-type component, as are the thermal output (heat output generated) for both the ohmic control and the preloaded NANOR[®]-type component. Four complete cycles are shown.

The graph in Figure 2, as in each of the other figures, shows first the response of the ohmic control, and then the response of the NANOR, the second ohmic control, and so on. Each of the outputs is read off from the right hand side. A pair of short calibration pulses is used for accuracy and precision checks of voltages and currents which are also shown between each set of measurements.

Compare the output for NANOR[®]-type LANR component to the thermal (ohmic) control. Figure 2 clearly demonstrates the larger differential incremental increase in temperature ($^{\circ}\text{C}$) for the NANOR[®] compared to the ohmic control. Attention is directed to the fact that the active preloaded LANR quantum electronic component clearly shows a larger, significant improvement in differential thermal output compared to a standard ohmic control (a carbon composition resistor). That amount of differential temperature increase for the preloaded NANOR[®]-type component heralds great utility for the energy output as a heat source.

Figure 3 is a set of curves which plot the temperature rise (delta- $T^{\circ}\text{C}$) of the preloaded NANOR[®]-type LANR component and the ohmic control normalized to input electrical power. These curves plot the temperature rise normalized to input electrical power as a function of time, so that the ratios can be used to estimate incremental power gain.

Figure 3 presents the differential temperature rise normalized to input electrical power for the preloaded NANOR[®], for the case with no input power ('background'), and for input to the ohmic thermal control, located at the core. The x -axis represents time, and each count represents 4 sec. The y -axis on the left side represents electrical input power (in watts). Each of the outputs is read off from the right-hand side. The y -axis on the right side represents the temperature rise (differential temperature increase) normalized (that is, divided by) to the electrical input power. The units of this axis are in $^{\circ}\text{C}/\text{W}$. Calibration pulses, used for accuracy and precision checks of voltages and currents, are also shown.

The NANOR[®] component and the ohmic control received four levels of input electrical power. Each is shown with its thermal output response to its electrical input. Almost five complete cycles are shown with their thermal output response to electrical input. Compare the delta- T output normalized to input power for preloaded NANOR[®]-type LANR component to the thermal (ohmic) control. Observe that despite lower input electrical power to the NANOR[®], the temperature rise normalized to input electrical power observed in the core is higher than expected, compared to the ohmic control. Note that the active

preloaded LANR quantum electronic component again clearly shows significant improvement in thermal output, here input-power-normalized compared to a standard ohmic control (a carbon composition resistor). Figure 3 heralds the excess energy achieved by the series VI NANOR[®] type of LANR component. It can be seen that the input power normalized delta measurements suggest strongly the presence of excess heat; a matter of great utility.

Figure 4 shows the input power and output heat flow normalized to input electrical power of a self-contained CF/LANR quantum electronic component NANOR 6-33. Figure 4 is a set of curves which plot the heat flow, normalized to input electrical power, leaving the system while driving the preloaded NANOR[®]-type LANR component and the ohmic control at four different electrical input powers. The heat flow is in response to the electrical input. It is an entirely different sensor from those used to determine dT/P_{in} or calorimetry. Figure 4 presents the output heat flow for the preloaded NANOR, for the case with no input, and for the ohmic thermal control, located at the core of the calorimeter. Four complete cycles of control of CF/LANR are shown. The x -axis represents time, and each count represents 4 sec. The y -axis on the left-hand side represents the electrical input power (in watts). The y -axis on the right side represents the heat flow output normalized (that is, divided by) to the electrical input power. Calibration pulses, used for accuracy and precision checks of voltages and currents, are also shown.

In Figure 4, compare the output heat flow normalized to input power for NANOR[®]-type LANR component with that for the thermal (ohmic) control. The long-term heat-flow measurements (using calibrated components) confirm the presence of excess energy, and validate the other measurements. It can be seen that despite lower input electrical power to the NANOR, the heat flow leaving the volume in which was contained, when normalized to the input electrical power, was higher than expected compared to the ohmic control. This was largest at lower input power levels. The response of the NANOR[®]-type LANR component is consistent with efficient energy gain, with the energy output as heat. The changes of the output with input power are consistent with the optimal operating point manifold of the LANR material. Therefore, the figure heralds the great efficiency of, and the excess energy coming from, the preloaded NANOR[®]-type of LANR component. Attention is directed to the fact that the active preloaded LANR quantum electronic component again clearly shows significant improvement in energy generated compared to a standard ohmic control (a carbon composition resistor) by this method too using heat flow. This information corroborates the marked and substantive incremental increase in energy output as heat for the preloaded NANOR[®]-type of LANR component.

Figure 5 depicts the electrical power input and thermal power output of a two-terminal NANOR[®]-type series

6-33 component, showing the calorimetric response at several input powers, for the ohmic control and the component. Four complete cycles are shown. The figure shows curves which plot the electrical input power, at four different input electrical power levels, and the calorimetric responses of both the ohmic control and the preloaded NANOR[®]-type component. Four complete cycles are shown. The *x*-axis represents time, and each count represents 4 sec. The *y*-axis on the left side represents electrical input power (in watts). The *y*-axis on the right side represents the amount of energy released. The units of this axis are in joules. The figure shows the input, and the calorimetry, of preloaded NANOR along with those for the ohmic thermal control used to calibrate the system. The calibration pulses, used for accuracy and precision checks of voltages and currents and time are also shown. The inputs to the thermal ohmic control, followed by the preloaded NANOR[®]-type component, are shown, as are the calibrated calorimetric outputs for both.

Each of the power and energy outputs is read off from the left- and the right-hand sides respectively. The latter curves (on the right-hand side axis) represent time integration to determine total energy. They thus rule out energy storage, chemical sources of the induced heat, possible phase changes and other sources of possible false positives. Compare the output for NANOR[®]-type LANR component to the thermal (ohmic) control. As can be seen, this semi-quantitative calorimetry, itself calibrated by thermal waveform reconstruction, is consistent with excess heat being produced only during energy transfer to the NANOR[®]-type LANR component.

Notice that the active preloaded LANR quantum electronic component clearly shows significant improvement in thermal output compared to a standard ohmic control (a carbon composition resistor). The graph, taken after the MIT IAP January 2012 class, is representative of the NANOR-type of CF/LANR technology, and shows nearly reproducible over unity thermal output power from the demonstration-power-level NANOR-type cold fusion (LANR) component.

Conclusion – utility and performance of NANOR[®]-type CF/LANR components

Dry, preloaded ZrO₂-PdNiD NANOR[®]-type CF/LANR components are capable of significant energy gain over long periods of time with reasonable reproducibility and controllability. The CF/LANR/CF activation is separated from its loading.

One such preloaded NANOR[®]-type CF/LANR component (a series VI type) was openly demonstrated at MIT, during and after, the IAP course on 30 and 31 January 2012. It demonstrated reproducible and controllable energy gain which ranged generally from 5 to 16+ (energy

gain of ~14.1 during the course demonstration; higher later) with energy and incremental power gains confirmed by three methods and time integration. It had an improved controlling/driving system which provided a reliable low power, high-efficiency, energy production component for demonstration and teaching purposes of size smaller than a centimetre, with an active site weight of less than 50 mg. Although small in size, this is actually not *de minimus* because the LANR excess power density is more than 19,500 W/kg of nanostructured material^{4,5}. The carbon footprint is zero, and the next generation will have higher power and ultimately produce electricity.

Possible future of clean, high performance energy production components

It is clear that these preloaded nanostructured NANOR[®]-type CF/LANR quantum electronic components are useful. They have shown significant improvement over their predecessors, including the highly successful metamaterial PHUSOR[®]-type of LANR component. This can be used as an effective, clean, highly efficient, energy production system, apparatus and process. Could these dry, preloaded, ready-to-be-activated, NANOR[®]-type LANR components/systems/materials, including in preassembled IC components and systems, be the future of clean and efficient energy production?

1. Swartz, M. Survey of the observed excess energy and emissions in lattice assisted nuclear reactions. *J. Sci. Exp.*, 2009, **23**(4), 419–436.
2. Swartz, M., LANR nanostructures and metamaterials driven at their optimal operating point. *J. Condens. Matter Nucl. Sci.*, 2012, **6**, 149; www.iscmns.org/CMNS/JCMNS-Vol6.pdf
3. Miles, M. *et al.*, Correlation of excess power and helium production during D₂O and H₂O electrolysis using palladium cathodes. *J. Electroanal. Chem.*, 1993, **346**, 99–117.
4. Swartz, M., Verner, G. and Tolleson, J., Energy gain from preloaded ZrO₂-PdNi-D nanostructured CF/LANR quantum electronic components. *J. Condens. Matter Nucl. Sci.*, 2014, **13**, 528; www.iscmns.org/CMNS/JCMNS-Vol13.pdf
5. Swartz, M. and Hagelstein, P. L., Demonstration of energy gain from a preloaded ZrO₂-PdD nanostructured CF/LANR quantum electronic component at MIT. *J. Condens. Matter Nucl. Sci.*, 2014, **13**, 516; www.iscmns.org/CMNS/JCMNS-Vol13.pdf
6. Arata, Y. and Zhang, Y. C., Observation of anomalous heat release and helium-4 production from highly deuterated palladium fine particles. *Jpn. J. Appl. Phys.*, 1999, **38**, L774-L776, Part 2, No. 7A.
7. Allard, L. F., Voelkl, E., Kalakkad, D. S. and Datye, A. K., Electron holography reveals the internal structure of palladium nanoparticles. *J. Mater. Sci.*, 1994, **29**(21), 5612–5614.

ACKNOWLEDGEMENTS. We thank Alex Frank, Alan Weinberg, Allen Swartz, Larry Forsley, Frank Gordon, Brian Ahern, Jeff Driscoll, Linda Hammond, Charles Entenmann and Andrew Meulenberg for their suggestions. This effort was supported by JET Energy Inc. and New Energy Foundation. NANOR[®] and PHUSOR[®] are registered trademarks of JET Energy, Incorporated. NANOR[®]-technology and PHUSOR[®]-technology are protected by US Patents D596724, D413659 and several other patents pending.